Research Article (Member)

Abaloparatide, a PTH Receptor Agonist with Homology to PTHrP, Enhances Callus Bridging and Biomechanical Properties in Rats with Femoral Fracture[1]

Beate Lanske,[1*] Heidi Chandler[1], Allen Pierce[1], Jeffery Brown[1], Michael Ominsky[1], Paul Kostenuik,[2] and Gary Hattersley[1]

[1]Radius Health Inc., Waltham, MA, USA

[2]University of Michigan School of Dentistry; Phylon Pharma Services, Newbury Park, CA, USA

Some of these data were presented in abstract form at the annual meeting of the American Society for Bone and Mineral Research in Denver, CO, USA, Sept. 8 – 11, 2017; and at the annual meeting of the American Association of Orthopedic Surgeons in New Orleans, LA, USA, March 6 – 10, 2018.

*****Correspondence:
Beate Lanske, PhD
Executive Director, Pre-Clinical Science
Radius Health
950 Winter Street
Waltham, MA 02451
Office: (617) 444-1907
Cell: (781) 775-0696
blanske@radiuspharm.com

Running title: Abaloparatide increases fracture callus strength

[1] This is the author manuscript accepted for publication and has undergone full peer review but has not been through the copyediting, typesetting, pagination and proofreading process, which may lead to differences between this version and the Version of Record. Please cite this article as doi:10.1002/jor.24254

Author contributions: HC, AP, JB, and GH conceived of and designed the study, with guidance from MO; HC, BL, MO, and PK analyzed the data and wrote the manuscript. All authors read and approved the final submitted manuscript.

Abstract

Fractures typically heal via endochondral and intramembranous bone formation, which together form a callus that achieves union and biomechanical recovery. PTHrP, a PTH receptor agonist, plays an important physiological role in fracture healing as an endogenous stimulator of endochondral and intramembranous bone formation. Abaloparatide, a novel systemically-administered osteoanabolic PTH receptor agonist that reduces fracture risk in women with postmenopausal osteoporosis, has 76% homology to PTHrP, suggesting it may have potential to improve fracture healing. To test this hypothesis, ninety-six 12-week-old male rats underwent unilateral internally-stabilized closed mid-diaphyseal femoral fractures and were treated starting the next day with daily s.c. saline (Vehicle) or abaloparatide at 5 or 20 μg/kg/d for 4 or 6 weeks (16 rats/group/time point). Histomorphometry and histology analyses indicated that fracture calluses from the abaloparatide groups exhibited significantly greater total area, higher fluorescence scores indicating more newly-formed bone, and higher fracture bridging scores versus Vehicle controls. Callus bridging score best correlated with callus cartilage score (r=0.64) and fluorescence score (r=0.67) at week 4, and callus area correlated with cartilage score (r=0.60) and fluorescence score (r=0.89) at week 6. By micro-CT, calluses from one or both abaloparatide groups had greater bone volume, bone volume fraction, bone mineral content, bone mineral density, and cross-sectional area at both time points versus Vehicle controls. Destructive bending tests indicated greater callus maximum load and stiffness in one or both abaloparatide groups at both time points versus Vehicle controls. These results provide preliminary preclinical evidence for improved fracture healing with systemically-administered abaloparatide.

Keywords: Fracture healing, cartilage, osteogenesis, orthopedics, bone formation, osteoporosis

Introduction

Fracture healing is usually a robust process that restores a broken bone's original strength and geometry.[1] Several endogenous factors are involved in orchestrating the multi-step process leading to successful fracture healing,[2] including parathyroid hormone-related protein (PTHrP).[3] Throughout much of the fracture healing cascade, numerous mesenchymal cell types increase their expression of PTHrP, including osteoblasts engaged in intramembranous ossification and chondrocytes involved in endochondral ossification.[4-6] PTH1R, the receptor for PTHrP and PTH, is also highly expressed by osteoblasts and chondrocytes during fracture healing,[4] and PTH1R mediates the anabolic responses to locally-upregulated PTHrP expression. The genetic ablation of PTHrP or PTH impairs long bone fracture healing in mice,[5; 7] and the systemic delivery of recombinant or synthetic forms of PTHrP and other PTH1R ligands, including full-length PTH(1-84) and its active amino-terminal fragment PTH(1-34), promotes fracture healing in animals.[3] Systemically-administered PTH(1-34) has also been shown to favorably influence some aspects of fracture healing in humans.[3]

Clinically, the goals of fracture healing are to restore biomechanical properties of the fractured bone and to facilitate the return of the affected limb or region to normal physiological function,[8] and attainment of these goals can be slow with certain fracture types and patient characteristics. Lower-limb long bone fractures sometimes lead to prolonged disability, and evidence indicates that around one third of working-age patients do not return to work within 12 months after a hip fracture.[9] Pharmacological interventions that accelerate fracture healing can substantially lower the overall costs associated with fractures by accelerating the return to work.[10] Among patients with open long bone fractures, as many as 25% may develop delayed union or nonunion,[11] which can cause major loss of productivity, decreased quality of life, and extensive health care utilization.[12-14] Despite clear unmet clinical needs, no pharmacological agents are currently

approved for the acceleration of fracture healing or for the treatment of delayed or nonunion fractures.[3; 15] Recombinant human bone morphogenetic protein-2 (rhBMP-2) mixed with an absorbable collagen sponge (ACS) is indicated for the acute treatment of tibial shaft fractures,[16] but this combination 'device' product is associated with several safety issues and is only indicated for the treatment of tibial fractures that have accessible fracture lines.[17] There remains an unmet need for agents that can enhance the healing of open and closed fractures, and systemically-administered bone anabolic agents have the potential to fulfill some of these needs.[18] Systemic agents can be delivered to patients with open or closed fractures, including fractures that are managed conservatively. Systemic agents may also have utility for treating fractures after definitive wound closure, which holds promise for the conservative management of fractures that develop signs of delayed healing.

Based on the important role of endogenous PTHrP as a mediator of fracture healing, pharmaceutically-active versions of PTHrP and PTHrP analogs have been tested and shown capable of promoting fracture healing in animals via their systemic administration.[19; 20] Abaloparatide is a novel subcutaneously-administered PTH1R agonist with 76% amino acid homology to PTHrP(1-34), and its daily administration to non-fractured rats and non-human primates increases bone formation, bone mass, and bone strength without increasing bone resorption.[21-25] Abaloparatide is currently approved by the U.S. Food and Drug Administration (FDA) as a treatment for postmenopausal osteoporosis based on its ability to reduce vertebral and non-vertebral fracture risk.[26] Due in part to its sequence homology with PTHrP, we hypothesized that abaloparatide will mimic or amplify some of the chondrogenic and/or osteogenic effects of endogenous PTHrP during fracture healing, potentially leading to improvements in callus bridging and biomechanical stability. Results from a recent femoral

osteotomy study showed that 28 days of abaloparatide administered to mice at a single high dose was associated with greater callus bone volume, but callus histology was not evaluated and treatment effects on callus biomechanics were inconclusive due to high variability and relatively small sample sizes.[27] The current report describes the effects of two dose levels of abaloparatide at two timepoints on callus histology, densitometry, and biomechanics in rats with a closed femoral fracture. This commonly used fracture model[28] was selected based on its reliance on chondrogenic and osteogenic healing, and calluses were assessed at the early-to-intermediate healing timepoints of 4 and 6 weeks to determine whether abaloparatide accelerates biomechanical recovery during the period when calluses have yet to fully regain normal femur strength.

Materials and Methods

Animal care and surgery

All animal procedures and activities were approved by and performed in an AAALAC-accredited vivarium at PharmaLegacy Laboratories (Shanghai, China). A total of 135 male Sprague-Dawley rats were purchased from Vital River Laboratory Animal Technology Company (Beijing, China) at 8-9 weeks of age, including 96 initial study animals plus 39 spares for cases when the location or morphology of experimental fractures were unsatisfactory. Animals underwent a health inspection upon arrival and were acclimated two per cage for at least 7 days in clear polycarbonate plastic cages (40 by 24 by 20 cm). Acclimated animals were singly-housed in a vivarium with a temperature range of 16-26 °C, relative humidity of 40-70%, and a 12-h light/dark cycle. Animals had free access to standard rodent chow (Shanghai SLAC Laboratory Animal Company) and filtered municipal tap water.

At approximately 12 weeks of age, rats were randomized into 3 groups of 32 animals each using an algorithm that minimized between-group differences in body weight (BioBook V10.0). Animals were anaesthetized by isoflurane inhalation and their right hind limb shaved and cleaned for the creation of a closed, internally-stabilized mid-diaphyseal fracture, as described previously.[28] Briefly, a medial peri-patellar incision was made, the patella was laterally displaced, and a sterile 20-gauge needle was inserted through the trochlear groove into the marrow cavity. The needle was removed and a sterile 1.2 mm diameter Kirschner wire (~27 mm long) was inserted to occupy most of the length of the medullary canal. The pinned femur was then positioned on a 3-point bending device and a single 700 g weight was dropped onto the femoral mid-diaphysis from a height of 25 cm to create a transverse fracture, which was confirmed by Faxitron X-ray images while the animals remained anesthetized. Buprenorphine HCl (0.05 mg/kg, i.m.) was administered for pain and gentamicin (20 mg/kg, i.m.) for infection control. Animals exhibiting improper pin placement, or unduly comminuted or poorly located fractures were euthanized by CO_2 plus cervical dislocation or cardiac exsanguination, and animals from the pool of 39 spare rats underwent the fracture protocol to achieve a final n of 32 fractured animals per treatment group. Animals were allowed to fully weight-bear after recovery from anesthesia. Animals were weighed at least once per week as a health-monitoring measure and for weight-based treatment dosing adjustments, and were observed daily to assess general health, recovery from surgery, and reactions to treatment.

Treatments, radiography, and sample sizes

One day after surgery, animals began receiving daily s.c. injections of 0.9% sodium chloride (Veh) or abaloparatide (Radius Health) at 5 (ABL5) or 20 µg/kg (ABL20) in a volume of 1 mL/kg. The abaloparatide dose levels were based on evidence of their tolerability and efficacy

over a 6-week treatment period in ovariectomized rats.[21] All animals were injected s.c. with the fluorochrome label calcein (10 mg/kg; Sigma Aldridge) 8 and 2 days prior to sacrifice.

Fracture site microradiographs were obtained at the start of treatment and weekly thereafter until necropsy for evaluations of callus formation and healing progress. Sixteen animals from each of the three treatment groups were sacrificed after 4 weeks and 6 weeks of treatment by CO_2 plus cervical dislocation or cardiac exsanguination. The number of animals (16 per group per time point) was chosen to provide 12 fracture samples for biomechanical analyses and 4 samples for histology.

Sample collection and evaluation

Fractured femurs were carefully harvested from all animals during scheduled necropsies. Twelve randomly-selected fractured femurs per group were wrapped in saline-soaked gauze and stored at -20°C prior to micro-CT and biomechanical assessment; contralateral femurs from these animals were similarly stored. The remaining 4 fractured femurs per group were fixed in 10% neutral buffered formalin for at least 48 h and stored in 70% alcohol prior to micro-CT and processing for histomorphometry and histology. Intermedullary pins were carefully removed prior to micro-CT scanning in all cases.

Micro-CT

Fractured femurs were scanned on a SkyScan 1176 system with the following settings: voltage 65 kV; current 385 μA; exposure 300 ms; rotation 0.7° per step (197.40° total); with images reconstructed to a nominal 18 μm isotropic voxel size. The region of interest (ROI) comprised a 350-slice area (slice thickness, 17.5 μm, 6.13mm total height) encompassing the fracture callus symmetrically about its midline, with semi-automated contouring used to delineate its periosteal

extent. The quantitative analysis of the ROI included the unthresholded parameters callus volumetric bone mineral content (vBMC), callus cross-sectional area (CSA), and callus regional volumetric bone mineral density (vBMD). In addition, a threshold of 100 was applied to determine total callus bone volume (BV) and bone volume fraction (BVF). In both cases, no delineation was made between the newly formed callus and the original cortex. After scanning, all femurs were returned to their original storage conditions prior to biomechanical or histologic examination.

Callus histology and histomorphometry

After fixation, histology samples were further dehydrated via a graded alcohol series using a Shandon Excelsier^{TM} tissue processor (Thermo-Fisher, Shanghai, China), then embedded in methylmethacrylate (Thermo Fisher). Two ~200 µm-thick slabs of the callus and adjacent bone were harvested parallel to the long bone axis using a saw (EXAKT, Germany) and ground to ~50 µm thickness using an EXAKT grinder (EXAKT). One unstained section was viewed under fluorescence microscopy to assess the extent of newly-formed calcein-labeled bone within the callus; semi-quantitative callus fluorescence scores were generated in a blinded manner on a scale of 0 to 4 (0 = none; 1 = mild; 2 = moderate; 3 = moderate-to-marked; 4 = marked). The other section was stained with toluidine blue (pH 6.5) for light microscopy analyses, which included photomicrographs, blinded semi-quantitative histology assessments, and quantitative bone histomorphometry. Semi-quantitative bridging scores (scale of 0 to 4) were determined in a binary manner by evaluating the presence or absence of contiguous bony or cartilaginous bridging across the periosteum and endocortex. Each of the two periosteal and endocortical surfaces were scored, with a maximum score of 4 indicating that all four evaluated surfaces were bridged. Semi-quantitative cartilage scores were determined by evaluating the extent of callus

cartilage (scale of 0 to 4, as described above) within each of the two callus regions on each section; scores for the two regions were averaged, leading to a maximum possible score of 4. The stained sections were also used for histomorphometric assessment of total external callus area (including bone, cartilage, and other tissue) using OsteoMeasure Software (Osteometrics, Decatur, GA, USA).

Biomechanical assessment of fractured and unfractured femurs

After thawing, fractured and unfractured femurs were tested in three-point bending using an MTS-858 Mini Bionix test system. Femurs underwent bending to failure at a displacement rate of 6 mm per minute with span length of 1 cm. Load and displacement data were used to determine maximum load and stiffness for each sample.

Statistics

One-way ANOVA was used to evaluate differences among the groups at each time point. If the ANOVA test was significant, Dunnett's post-test was applied to compare the ABL5 and ABL20 groups to Veh controls within each time point. For the qualitative callus fluorescence and cartilage scores, the non-parametric Kruskal-Wallis test was used to compare overall group differences at each time point, followed by Dunn's multiple comparison test of each ABL group vs Veh control if Kruskal-Wallis was significant. These analyses and linear regressions were performed using GraphPad Prism V7.03, with a P value of <0.05 used to indicate statistically significant differences.

Results

Callus radiography

Radiographs of the fractured femur were obtained from anaesthetized animals at the time of fracture (week 0) and once-weekly thereafter. Representative radiographs taken at weeks 0, 2, 4, and 6 from the 6-week arm of the study are shown in Fig. 1. In all three groups, substantial callus development was evident by week 2, with an apparent increase in callus density at week 4. Calluses appear to be denser in the ABL5 and ABL20 groups compared with Veh controls at weeks 4 and 6.

Callus Histology and Histomorphometry

Representative photomicrographs of undecalcified toluidine blue-stained histology sections of week 4 and week 6 fracture calluses are presented in Fig. 2, and the following interpretations are consistent with observations for the overall histology sample set. At week 4, all three groups show substantial external callus development in the form of new intramembranous bone along the upper and lower periosteal surfaces; smaller and variable degrees of internal callus development are evident in the form of new intramedullary bone. The week 4 abaloparatide examples (Fig. 2B-C) exhibit somewhat denser and more developed external calluses compared with Veh controls (Fig. 2A), with an apparently greater extent of purple-stained callus cartilage. At week 6, the abaloparatide groups (Fig. 2E-F) continue to exhibit greater amounts of new external and internal bony callus tissue compared with Veh controls (Fig. 2D). Callus cartilage is minimally evident in the Week 6 Veh and ABL5 examples, whereas the Week 6 ABL20 example exhibits moderate callus cartilage surrounded by external bony callus tissue.

Histomorphometry analyses indicated that total callus area was significantly greater in both abaloparatide groups at week 4 and in the ABL20 group at week 6 compared with Veh controls (Fig. 3A). Semi-quantitative histology assessments indicated a trend toward greater cartilage

scores at week 4 for the ABL20 group compared with Veh controls (p = 0.08; Fig. 3B). Callus fluorescence scores reflecting the extent of newly-formed bone were significantly higher in the ABL20 group at both time points compared with Veh controls (Fig. 3C). Callus bridging scores, reflecting cartilaginous and/or bony bridging across the fracture line, were significantly greater in both abaloparatide groups at week 4 compared with Veh controls, with similar levels of bridging for each group at week 6 (Fig. 3D).

Linear regression analyses were performed to evaluate histological determinants of bridging scores and callus area (Table 1). Bridging score was positively related to cartilage score and fluorescence score at week 4 (r = 0.64 and 0.67, respectively; both $P < 0.05$) but not at week 6. Callus area at week 4 was positively related to fluorescence score (r = 0.90; $P < 0.0001$), and callus area at week 6 was positively related to fluorescence score (r = 0.89) and to cartilage score (r = 0.60; $P < 0.05$).

Callus micro-CT

Quantitative micro-CT analyses of fractured femurs indicated that the ABL5 and ABL20 groups had significantly greater callus bone volume, BVF, and vBMC at both time points compared with Veh controls (Fig. 4A-C). The ABL5 group showed significantly greater average callus CSA at weeks 4 and 6 compared with Veh controls (Fig. 4D). Callus region vBMD was significantly greater in both abaloparatide groups at both time points compared with Veh controls (Fig. 4E). Representative 2-D reconstructed images are shown in Fig. 5.

Biomechanics of the callus and unfractured femur

Destructive 3-point bending tests of fracture calluses indicated significantly greater strength (maximum load) in the ABL20 group at week 4 and the ABL5 group at week 6 compared with

their respective Veh control groups (Fig. 6A). Callus stiffness was significantly greater for the ABL5 and ABL20 groups compared with Veh controls at week 4, and for the ABL5 group versus Veh at week 6 (Fig. 6B). Unfractured contralateral femurs were also subjected to destructive 3-point bending tests, which indicated significantly greater maximum load in the ABL20 group compared with Veh controls at week 4 (Fig. 6C). Stiffness values for intact femurs were similar across the three groups at weeks 4 and 6 (Fig. 6D).

The degree of biomechanical recovery of fractured femurs was assessed by calculating callus maximum load and stiffness values for each animal as a percentage of the average values for normal femurs (i.e., unfractured femurs from Veh controls). Calluses from the Veh group reached 24.0 ± 1.7% (mean ± SEM) and 7.4 ± 0.8% of normal maximum load and stiffness at week 4 (respectively), and at week 6 these values reached 35.0 ± 3.4% and 25.4 ± 3.9%, respectively. Calluses from the ABL5 group achieved 33.9 ± 3.8% and 11.8 ± 0.9% of normal maximum load and stiffness at week 4 (respectively), and at week 6 these values reached 49.2 ± 4.6% and 53.9 ± 7.7%, respectively (all $P < 0.05$ vs Veh except for week 4 maximum load). Calluses from the ABL20 group achieved 42.5 ± 4.0% and 14.5 ± 1.0% of normal maximum load and stiffness at week 4, respectively (both $P < 0.05$ versus Veh). Maximum load remained similar at week 6 in the ABL20 group (42.0 ± 4.7% of normal) compared with week 4, whereas stiffness was further increased at week 6 to 30.6 ± 6.4% of normal ($P < 0.05$ vs. Veh).

Micro-CT-based morphological determinants of callus biomechanics

Determinants of callus biomechanics were assessed across the 3 groups at each time point via linear regression analyses of micro-CT-derived callus morphology variables versus callus maximum load and stiffness. Callus CSA, vBMC, bone volume, and BVF were positively

correlated with maximum load and stiffness at week 4, with r values ranging from 0.64 to 0.81 (all $P < 0.05$; Table 1). At week 4, callus region vBMD was positively associated with stiffness but not with maximum load (r = 0.68; $P < 0.05$). At week 6, callus vBMC, vBMD, and BVF remained positively correlated with maximum load and stiffness (r values ranging from 0.34 to 0.76; all $P < 0.05$), whereas callus CSA and bone volume were no longer associated with maximum load or stiffness.

Discussion

This study provides preliminary evidence for accelerated fracture healing in animals treated with abaloparatide, a novel and selective PTH1R agonist with 76% homology to PTHrP. Previous animal studies show that genetic PTHrP deficiency reduces fracture callus chondrogenesis and bony callus development,[29] and that exogenous PTHrP and PTHrP analogs enhance fracture healing and osteotomy healing.[19; 20] A recent study in mice with closed femoral fractures also showed that 28 days of abaloparatide administration at a single high dose (60 μg/kg/d) led to significantly greater callus bone volume.[27] The current study shows that abaloparatide enhanced callus development, osteogenesis, fracture bridging, and biomechanical recovery during the early and middle stages of fracture healing in rats with a closed femoral fracture. These findings provide further preclinical evidence that abaloparatide may improve the healing of traumatic fractures, and perhaps fragility fractures as well.

Abaloparatide-treated rats exhibited larger calluses containing substantial amounts of cartilage, more bone, and enhanced bridging at week 4 compared with vehicle controls. These differences were accompanied by enhanced callus strength and stiffness, with some evidence for accelerated biomechanical recovery: namely, callus maximum load was greater in the ABL20 group at week

4 than in Veh controls at week 6. Abaloparatide appeared to enhance intramembranous bone formation emanating from periosteal surfaces adjacent to the fracture line, an effect that could potentially contribute to a more extensive rigid scaffold for subsequent bridging. Bridging is typically achieved in this model via the formation of callus cartilage between the banks of this new intramembranous bone, and the abaloparatide-treated rats exhibited trends toward increased callus cartilage, though statistical power was limited by the small number of histology samples. Positive correlations between callus cartilage and bridging scores suggest a possible contribution of chondrogenesis in fracture union.

In addition to its role in initial union, callus cartilage provides a template for subsequent endochondral-based bone formation that provides much of the biomechanical stability of the healing fracture.[3] The current study provides evidence for the timely conversion of callus cartilage to bone in all three groups, based on numerical reductions in cartilage scores between weeks 4 and 6 and accompanying increases in callus bone volume, vBMD, and vBMC. One or both abaloparatide groups also exhibited greater callus fluorescence scores, callus bone volume, and callus bone mineral content compared with Veh, which reflect the combined contributions of intramembranous and endochondral bone formation. Callus fluorescence scores correlated positively with total callus volume and with bridging scores, suggesting significant contributions of abaloparatide-induced osteogenesis toward bony callus development and bridging. However, it is important to note that improved bridging in the abaloparatide groups was seen only at week 4 and not at week 6, despite the fact that none of the groups had achieved complete bridging at week 6.

Consistent with the lack of complete bridging, destructive biomechanical testing of fracture calluses indicated that the Veh controls achieved around 25% and 35% of the strength and

stiffness of normal unfractured femurs by week 6. This degree of biomechanical recovery is similar to day 40 findings from another closed long-bone fracture study in rats,[30] and indicates an early-to-intermediate stage of healing. There are advantages to evaluating treatment effects on callus development at these stages, including mechanistic insights gained by evaluating callus cartilage before and after it begins converting into bone. There is also value in assessing callus biomechanics at these stages, because over longer treatment periods, callus strength can significantly exceed the strength of normal unfractured bone, which had debatable clinical value.[3] The current study showed that the one or both abaloparatide groups had greater callus strength and stiffness at weeks 4 and 6 vs Veh controls, with levels reaching up to around 50% of those observed for normal intact femurs. Future studies with longer follow-up periods may address whether abaloparatide reduces the time to achieve full callus biomechanical recovery.

Significant positive correlations were observed between several micro-CT-based callus structural parameters versus callus strength and stiffness. For some structural parameters (e.g., CSA and bone volume), relationships with callus biomechanics were evident at week 4 but not at week 6. This temporal shift may reflect the effects of callus remodeling, which reduces external callus size as internal repair processes progressively stabilize the healing fracture from within. Conversely, callus bone volume fraction and vBMD were better callus strength surrogates at week 6 than at week 4. These collective findings, and the histology-based regression analyses, suggest that callus cartilage, bone formation, and overall callus size and mass were the main determinants of early callus stability, with callus remodeling and maturity becoming more biomechanically relevant during the intermediate stages of healing.

The effects of abaloparatide on bone healing in this rat study are consistent with previous findings of favorable bone healing responses to exogenous PTHrP and other PTHrP analogs in

mice and rabbits with fractures or other skeletal injuries.[19; 20; 27; 31; 32] This study also has several limitations. A standard closed femoral fracture model was considered suitable for this initial abaloparatide study, but data from higher-hurdle fracture models would better inform the potential of abaloparatide as a possible treatment for fractures that do not readily heal on their own. The effects of abaloparatide were only assessed in male rats, and we cannot rule out that abaloparatide may have different effects on fracture healing in female rats. Cartilage scores were semi-quantitative and were based on Toluidine Blue-stained sections and should therefore be considered a preliminary assessment, pending quantitative analyses using stains that are more specific for cartilage matrix. The study lacked an active comparator group such as PTH(1-34) or BMP-2 therapy, and while neither of those therapies are approved for the treatment of closed long-bone fractures, it would nevertheless be interesting to compare their effects versus those of abaloparatide. Abaloparatide administration influenced unfractured bones as well, as shown by improved biomechanical properties of unfractured femurs. This effect was not unexpected and may be considered favorable in settings of low bone mass and strength, but such effects may be less desirable in patients who are not at increased risk of fragility fractures. It is assumed but unproven that effects on unfractured bones would gradually reverse after a completing a course of abaloparatide therapy for fracture healing.

In summary, abaloparatide administration to rats with a closed femoral fracture was associated with early increases in callus osteogenesis, improved fracture bridging, greater bony callus size and density, and improved biomechanical stability. We hypothesize that callus cartilage may have contributed to improved early bridging and callus stability in the abaloparatide groups, and that the timely conversion of this cartilage into bone, combined with abaloparatide-induced stimulation of intramembranous periosteal bone formation, may have further contributed to

increased callus strength and stiffness. From a clinical perspective, early improvements in fracture callus stability may allow earlier recovery of physical activities including weight-bearing, potentially leading to further improvements in fracture healing due to an early regain of mechanical loading. These current findings, and those from other experimental orthopedic models,[27] provide initial preclinical support for further studies of abaloparatide as an investigational agent for the promotion of bone healing.

Acknowledgements

Funding for this work was provided by Radius Health, which also provided study drug. Authors BL, HC, AP, JB, MO, and GH are current or former employees of Radius Health and may be Radius Health shareholders. Author PK owns shares in Radius Health and received funding support from Radius Health to provide medical writing assistance for this manuscript. We thank Frank Asuncion for helpful input regarding histology analyses, and Danfeng Liu, Mei-Shu Shih, and Yuan Hongjiang from PharmaLegacy, for their oversight of the in-life portion of the study.

References

1. Einhorn TA, Gerstenfeld LC. 2015. Fracture healing: mechanisms and interventions. Nat Rev Rheumatol 11:45-54.
2. Barnes GL, Kostenuik PJ, Gerstenfeld LC, et al. 1999. Growth factor regulation of fracture repair. J Bone Miner Res 14:1805-1815.
3. Kostenuik P, Mirza FM. 2017. Fracture healing physiology and the quest for therapies for delayed healing and nonunion. J Orthop Res 35:213-223.
4. Okazaki K, Jingushi S, Ikenoue T, et al. 2003. Expression of parathyroid hormone-related peptide and insulin-like growth factor I during rat fracture healing. J Orthop Res 21:511-520.

5. Wang M, Nasiri AR, Broadus AE, et al. 2015. Periosteal PTHrP Regulates Cortical Bone Remodeling During Fracture Healing. Bone 81:104-111.

6. Kakar S, Einhorn TA, Vora S, et al. 2007. Enhanced chondrogenesis and Wnt signaling in PTH-treated fractures. J Bone Miner Res 22:1903-1912.

7. Ren Y, Liu B, Feng Y, et al. 2011. Endogenous PTH deficiency impairs fracture healing and impedes the fracture-healing efficacy of exogenous PTH(1-34). PLoS One 6:e23060.

8. Goldhahn J, Scheele WH, Mitlak BH, et al. 2008. Clinical evaluation of medicinal products for acceleration of fracture healing in patients with osteoporosis. Bone 43:343-347.

9. Ekegren CL, Edwards ER, Oppy A, et al. 2017. Twelve-month work-related outcomes following hip fracture in patients under 65 years of age. Injury 48:701-707.

10. Alt V, Donell ST, Chhabra A, et al. 2009. A health economic analysis of the use of rhBMP-2 in Gustilo–Anderson grade III open tibial fractures for the UK, Germany, and France. Injury 40:1269-1275.

11. Westgeest J, Weber D, Dulai SK, et al. 2016. Factors associated with development of nonunion or delayed healing after an open long bone fracture: A prospective cohort study of 736 subjects. J Orthop Trauma 30:149-155.

12. Kanakaris NK, Giannoudis PV. 2007. The health economics of the treatment of long-bone non-unions. Injury 38 Suppl 2:S77-84.

13. Hak DJ, Fitzpatrick D, Bishop JA, et al. 2014. Delayed union and nonunions: epidemiology, clinical issues, and financial aspects. Injury 45 Suppl 2:S3-7.

14. Schottel PC, O'Connor DP, Brinker MR. 2015. Time trade-off as a measure of health-related quality of life: Long bone nonunions have a devastating impact. J Bone Joint Surg Am 97:1406-1410.

15. Dent-Acosta RE, Storm N, Steiner RS, et al. 2012. The tactics of modern-day regulatory trials. J Bone Joint Surg Am 94 Suppl 1:39-44.

16. http://www.accessdata.fda.gov/cdrh_docs/pdf/P000054b.pdf. 2004. FDA summary of safety and effectiveness data INFUSE(R) Bone Graft.

17. Carragee EJ, Hurwitz EL, Weiner BK. 2011. A critical review of recombinant human bone morphogenetic protein-2 trials in spinal surgery: emerging safety concerns and lessons learned. Spine J 11:471-491.

18. Bukata SV. 2011. Systemic administration of pharmacological agents and bone repair: what can we expect. Injury 42:605-608.

19. Bostrom MP, Gamradt SC, Asnis P, et al. 2000. Parathyroid hormone-related protein analog RS-66271 is an effective therapy for impaired bone healing in rabbits on corticosteroid therapy. Bone 26:437-442.

20. Liu A, Li Y, Wang Y, et al. 2015. Exogenous parathyroid hormone-related peptide promotes fracture healing in lepr(-/-) mice. Calcif Tissue Int 97:581-591.

21. Bahar H, Gallacher K, Downall J, et al. 2016. Six weeks of daily abaloparatide treatment increased vertebral and femoral bone mineral density, microarchitecture and strength in ovariectomized osteopenic rats. Calcif Tissue Int 99:489-499.

22. Doyle N, Varela A, Haile S, et al. 2018. Abaloparatide, a novel PTH receptor agonist, increased bone mass and strength in ovariectomized cynomolgus monkeys by increasing bone formation without increasing bone resorption. Osteoporos Int 29:685-697.

23. Varela A, Chouinard L, Lesage E, et al. 2017. One year of abaloparatide, a selective peptide activator of the PTH1 receptor, increased bone mass and strength in ovariectomized rats. Bone 95:143-150.

24. Varela A, Chouinard L, Lesage E, et al. 2017. One year of abaloparatide, a selective activator of the PTH1 receptor, increased bone formation and bone mass in osteopenic ovariectomized rats without increasing bone resorption. J Bone Miner Res 32:24-33.

25. Chandler H, Lanske B, Varela A, et al. 2018. Abaloparatide, a novel osteoanabolic PTHrP analog, increases cortical and trabecular bone mass and architecture in orchiectomized rats by increasing bone formation without increasing bone resorption. Bone 120:148-155.

26. Miller PD, Hattersley G, Riis BJ, et al. 2016. Effect of abaloparatide vs placebo on new vertebral fractures in postmenopausal women with osteoporosis: A randomized clinical trial. JAMA 316:722-733.

27. Bernhardsson M, Aspenberg P. 2018. Abaloparatide versus teriparatide: a head to head comparison of effects on fracture healing in mouse models. Acta Orthop:1-6.

28. Bonnarens F, Einhorn T. 1984. Production of a standard closed fracture in laboratory animal bone. J Orthop Res 2:97-101.

29. Wang YH, Qiu Y, Han XD, et al. 2013. Haploinsufficiency of endogenous parathyroid hormone-related peptide impairs bone fracture healing. Clin Exp Pharmacol Physiol 40:715-723.

30. Andreassen TT, Ejersted C, Oxlund H. 1999. Intermittent parathyroid hormone (1-34) treatment increases callus formation and mechanical strength of healing rat fractures. J Bone Miner Res 14:960-968.

31. Lozano D, de Castro LF, Dapia S, et al. 2009. Role of parathyroid hormone-related protein in the decreased osteoblast function in diabetes-related osteopenia. Endocrinology 150:2027-2035.

32. Lozano D, Fernandez-de-Castro L, Portal-Nunez S, et al. 2011. The C-terminal fragment of parathyroid hormone-related peptide promotes bone formation in diabetic mice with low-turnover osteopaenia. Br J Pharmacol 162:1424-1438.

Table 1: Callus morphology variables as determinants of callus bridging, area, strength (maximum load), and stiffness as determined by linear regression analyses. All listed r values are statistically significant ($P < 0.05$); NS, not significant.

	Correlation coefficients (r values)	
	Week 4	Week 6
Callus histology and histomorphometry (n = 4/group)		
Cartilage score vs bridging score	0.64	NS
Cartilage score vs callus area	NS	0.60
Fluorescence score vs bridging score	0.67	NS
Fluorescence score vs callus area	0.90	0.89
Callus micro-CT and biomechanics (n = 12/group)		
CSA vs max load	0.78	NS
CSA vs stiffness	0.64	NS
vBMC vs max load	0.69	0.35
vBMC vs stiffness	0.78	0.34
Bone volume vs max load	0.75	NS
Bone volume vs stiffness	0.81	NS
BVF vs max load	NS	0.53
BVF vs stiffness	0.64	0.76
vBMD vs max load	NS	0.54
vBMD vs stiffness	0.39	0.78

vBMC, volumetric bone mineral content; CSA, cross-sectional area; BVF, bone volume fraction; vBMD, volumetric bone mineral density.

Figure Legends

Figure 1: Representative radiographs of fracture calluses from the 6-week arm of the study. Examples were selected based on callus strength (maximum load) and stiffness values that were closest to their group means. Callus density in the ABL5 and ABL20 groups appears to be greater at week 4 and week 6 compared with Veh controls.

Figure 2: Representative histology of undecalcified toluidine blue-stained sections of fracture calluses. Examples were selected based on microCT-based callus bone volume values closest to their group means. The red dashed line in Fig. A indicates periosteal new bone formation that comprises much of the external callus, and the blue arrows indicate new endocortical bone formation that comprises the internal callus. The purple arrows in Figs. B and C highlight callus cartilage within the fracture gap between the external bony callus regions.

Figure 3: Histomorphometry- and histology-based callus analyses. A: Histomorphometry-based total callus area. B-D: Semi-quantitative histology-based analyses of (B) callus cartilage score, (C) callus fluorescence score, which reflects the extent of new bone formation within the external callus region; and (D) callus bridging score, which reflects contiguous cartilaginous and bony tissue that bridges the fractured ends. Data represent means and SEM, N = 4/group. *P < 0.05 vs Veh control group at the corresponding time point.

Figure 4: Fracture callus morphology by micro-CT. A) Callus bone volume; B) Callus bone volume fraction (% total volume); C) Callus volumetric bone mineral content (vBMC); D) Callus cross-sectional area (CSA); E) Callus region volumetric BMD (vBMD). Data represent means and SEM, n = 16/group. *P < 0.05 compared with Veh at the corresponding time point.

Figure 5: Representative micro-CT images of fracture calluses. Selection of these 2-D reconstructed images was based on samples with ultimate load values closest to their group means.

Figure 6: Biomechanics results for (A, B) fracture calluses and (C, D) unfractured intact contralateral femurs. Data represent means and SEM, n = 12/group. *P < 0.05 vs. Veh controls at the corresponding same time point.

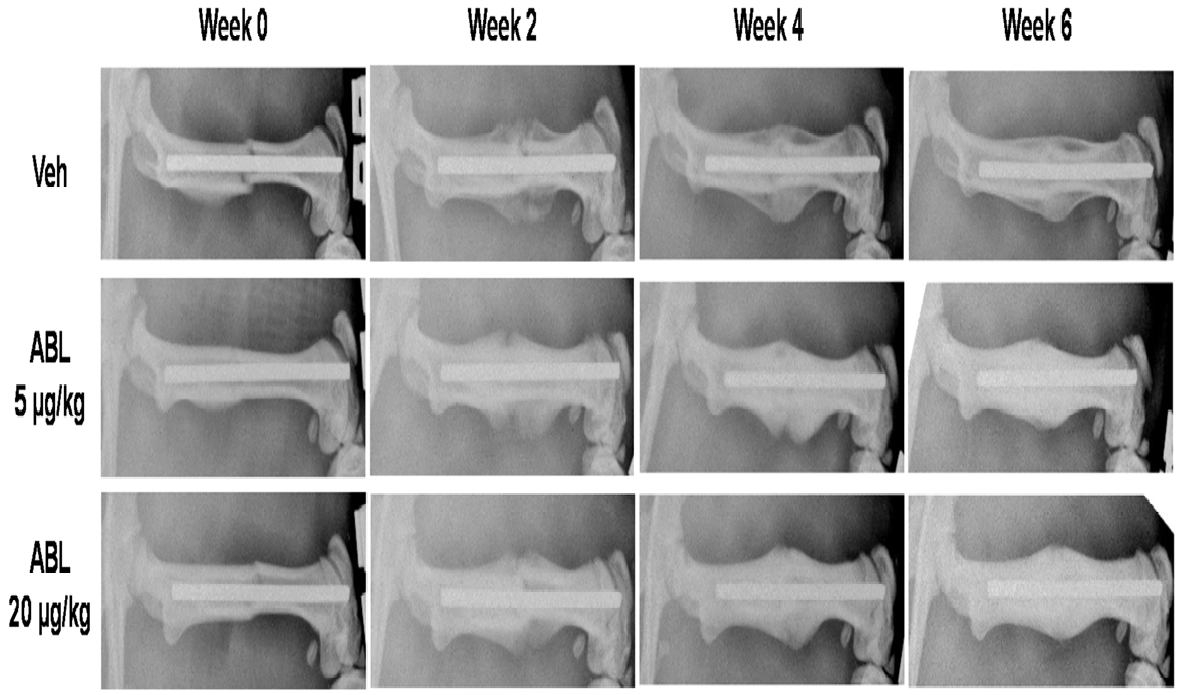

Figure 1 Radiographs .

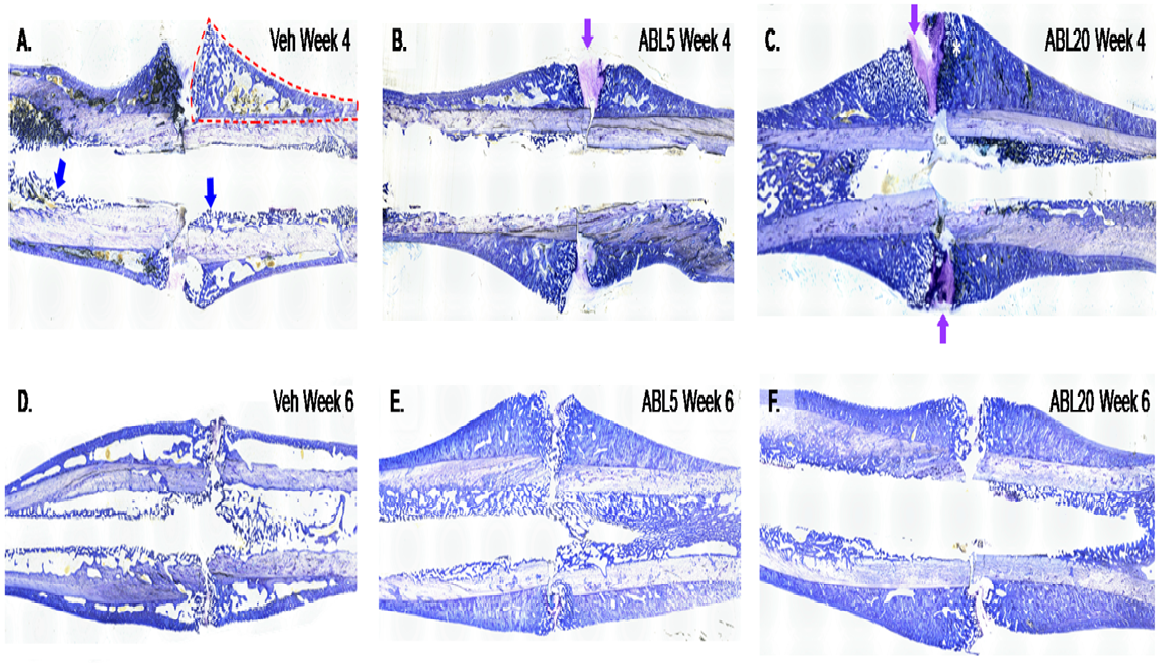

Figure 2 Callus photomicrographs .

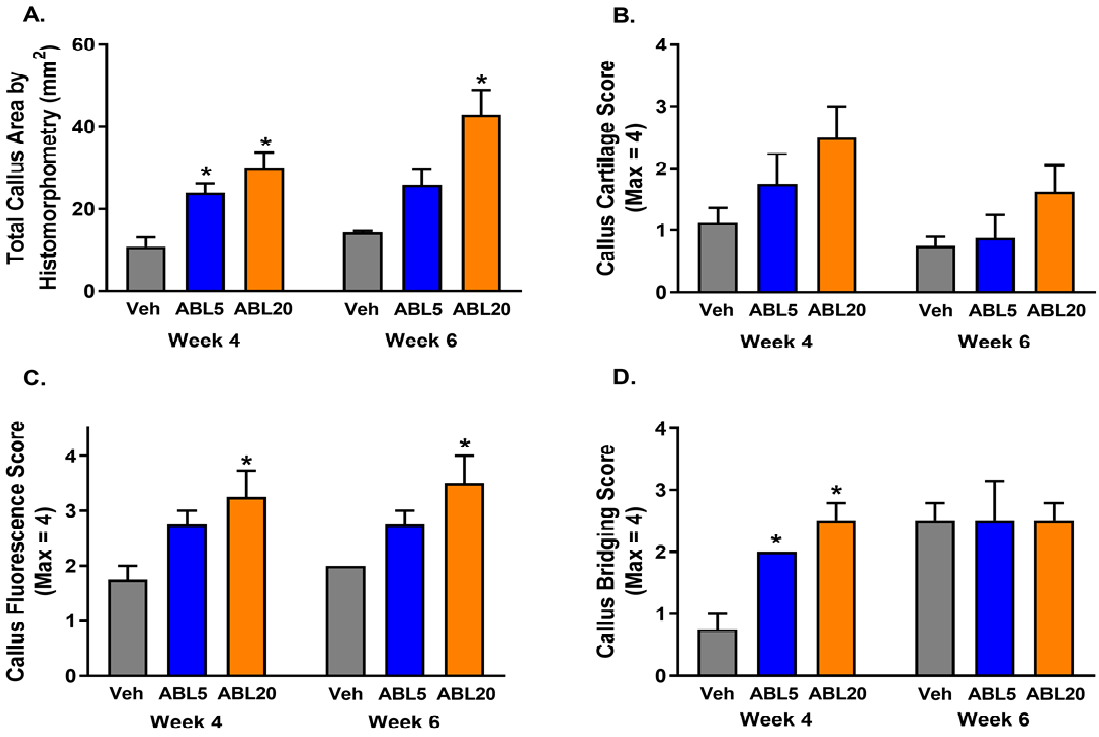

Figure 3 callus histomorphometry and histology .

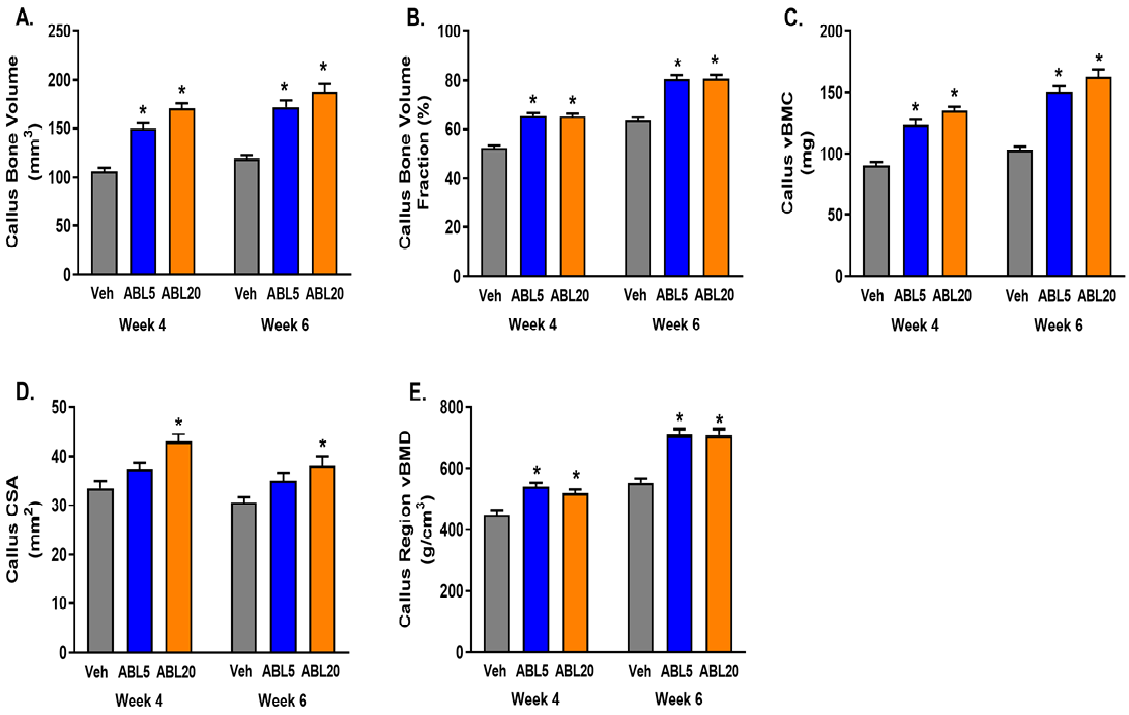

Figure 4 Callus micro-CT .

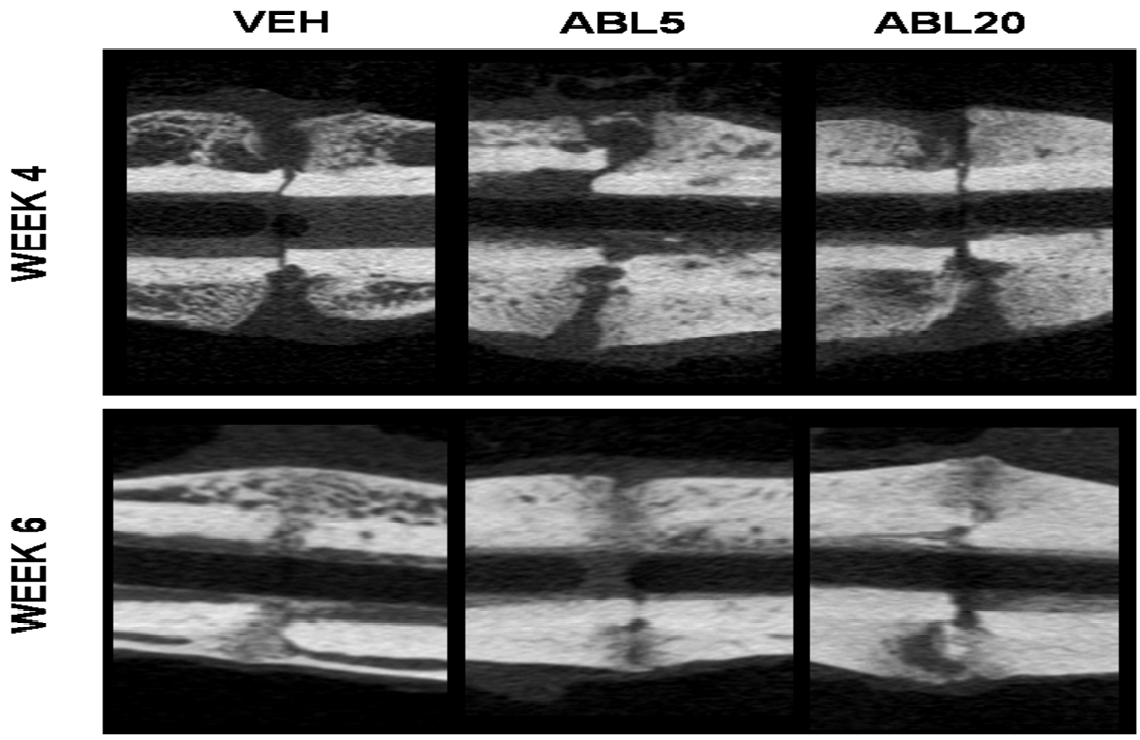

Figure 5 Micro-CT images .

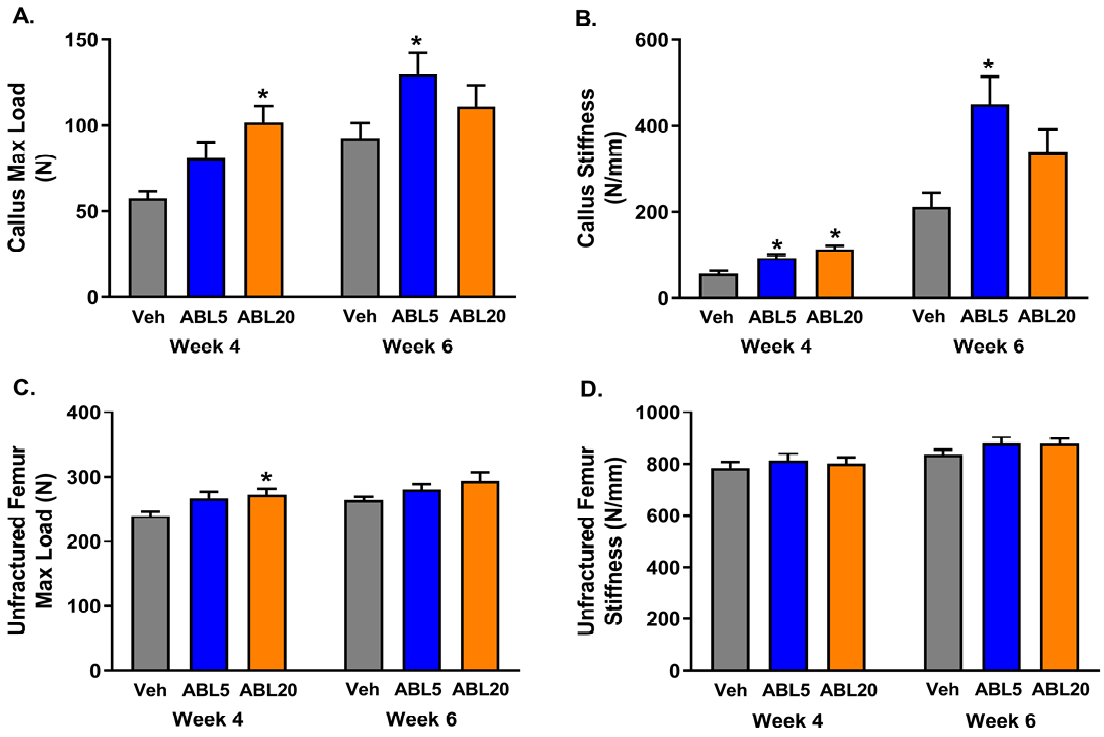

Figure 6 Biomechanics .